ACS APPLIED MATERIALS & INTERFACES

Research Article

www.acsami.org

Microscale Surface Modifications for Heat Transfer Enhancement

Huseyin Bostanci,*[,†,⊥] Virendra Singh,[‡,#] John P. Kizito,[§] Daniel P. Rini,[∥] Sudipta Seal,[‡] and Louis C. Chow[†]

[†]Department of Mechanical and Aerospace Engineering, University of Central Florida, Orlando, Florida 32816, United States

[‡]Department of Materials Science and Engineering, Advanced Materials Processing Analysis Center, Nanoscience Technology Center, University of Central Florida, Orlando, Florida 32816, United States

[§]Department of Mechanical Engineering, North Carolina Agricultural and Technical State University, Greensboro, North Carolina 27411, United States

[∥]RINI Technologies, Inc., Oviedo, Florida 32765, United States

ABSTRACT: In this experimental study, two surface modification techniques were investigated for their effect on heat transfer enhancement. One of the methods employed the particle (grit) blasting to create microscale indentations, while the other used plasma spray coating to create microscale protrusions on Al 6061 (aluminum alloy 6061) samples. The test surfaces were characterized using scanning electron microscopy (SEM) and confocal scanning laser microscopy. Because of the surface modifications, the actual surface area was increased up to 2.8× compared to the projected base area, and the arithmetic mean roughness value (R_a) was determined to vary from 0.3 μm for the reference smooth surface to 19.5 μm for the modified surfaces. Selected samples with modified surfaces along with the reference smooth surface were then evaluated for their heat transfer performance in spray cooling tests. The cooling system had vapor-atomizing nozzles and used anhydrous ammonia as the coolant in order to achieve heat fluxes up to 500 W/cm^2 representing a thermal management setting for high power systems. Experimental results showed that the microscale surface modifications enhanced heat transfer coefficients up to 76% at 500 W/cm^2 compared to the smooth surface and demonstrated the benefits of these practical surface modification techniques to enhance two-phase heat transfer process.

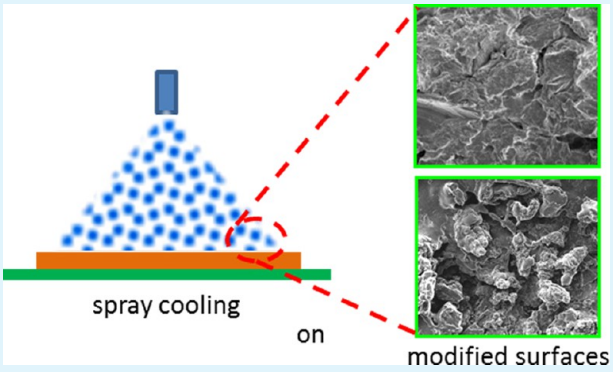

KEYWORDS: *surface modification, particle blasting, plasma spray, heat transfer enhancement, spray cooling*

1. INTRODUCTION

Surface characteristics have long been known to have an effect on boiling heat transfer enhancement, and various surface modification methods have been extensively investigated. These efforts were largely driven by the demanding applications, such as electronics cooling, that require efficient heat removal at ever increasing heat fluxes. Previous studies, as reviewed by Carey,[1] showed that the "nucleate boiling" is most effective when there exists an abundance of cavities on the surface to act as nucleation sites. These cavities are most likely to become active nucleation sites if they effectively entrap vapor and/or gas in them. Therefore, most widely studied ways of enhancing nucleate boiling have been (a) increasing the surface roughness and (b) creation of special surfaces featuring artificially-formed cavities designed to efficiently trap vapor. Two well-known textbooks by Webb and Kim[2] and Thome[3] provide comprehensive background knowledge and review of literature on enhanced surfaces. Some recent studies demonstrated new surface enhancement methods in pool boiling heat transfer. El-Genk and Ali[4] developed electrochemically deposited copper dendritic microstructures for tests in PF-5060. Yang et al.[5] investigated copper foam structures with varying porosity and thickness in water. Tang et al.[6] tested nanoporous copper surfaces fabricated by the facile hot-dip galvanizing/dealloying process in water. Wu et al.[7] studied hydrophilic TiO_2 nanoparticle modified surface in water and FC-72, and Betz et al.[8] characterized superhydrophilic, superhydrophobic, and superbiphilic surfaces, made by applying a combination of random nanostructuring processes, microlithography, and thin hydrophobic polymer coating, in water.

The current study focuses on practical surface modification methods that could be adopted in emerging thermal management applications, such as high-power laser diode arrays in military tactical platforms and power electronics in hybrid electric vehicles, that require high heat flux removal with acceptable device temperatures. Moreover, these applications strive for compact, lightweight, and energy efficient system designs. In this work, a spray cooling system was utilized to

Received: June 27, 2013
Accepted: September 4, 2013
Published: September 4, 2013

   dx.doi.org/10.1021/am402512f | ACS Appl. Mater. Interfaces 2013, 5, 9572−9578

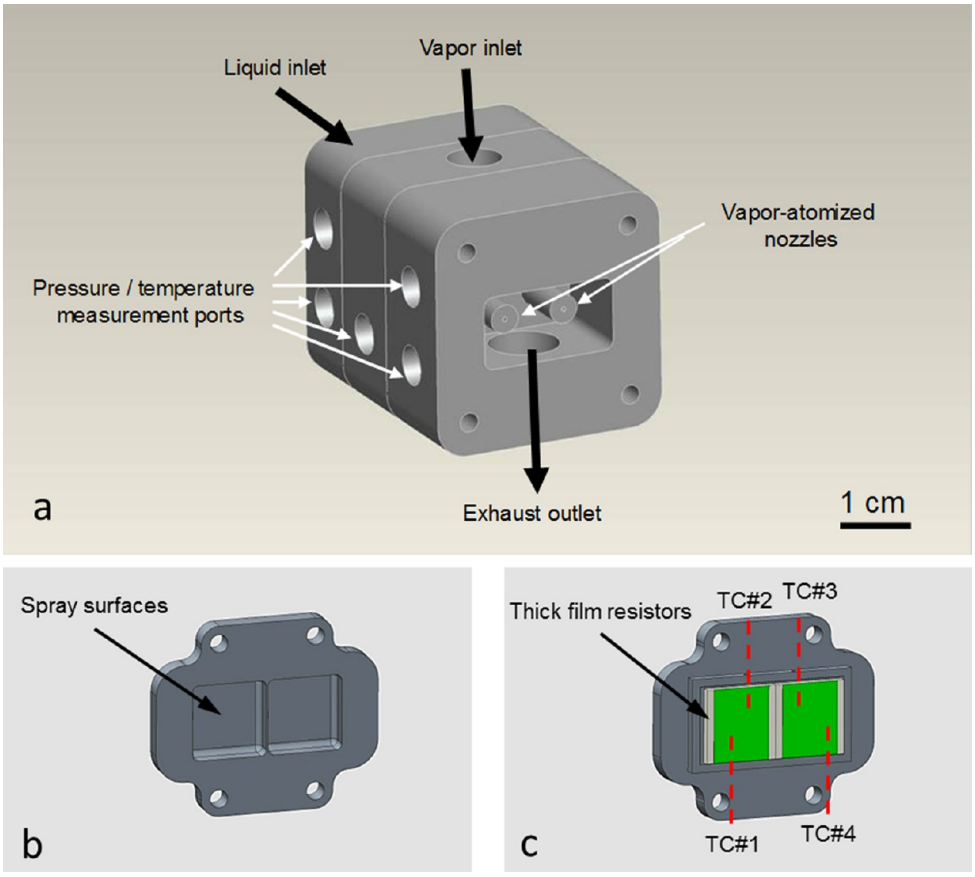

Figure 1. Spray cooling module with liquid, vapor, and spray/exhaust manifolds and spray nozzles (a), heater sample-spray side (b), heater sample-resistor side (c).

evaluate the test surfaces at heat fluxes up to 500 W/cm^2. The spray cooling involves nucleate boiling as one of its major heat transfer mechanisms. Some models can be used as guidelines in designing surface characteristics. The model developed by Hsu[9] can roughly predict the range of active cavity sizes in nucleate boiling as a function of surface superheat that is defined as the difference between the surface temperature and the pool saturation temperature. Considering the thermophysical properties of the coolant, i.e., ammonia, in this study, and a 7 °C surface superheat level, the cavity mouth radius in the predicted range of active cavities spans between 0.35 and 1.40 μm.[10] When the geometry of a real cavity is idealized as a conical shape, the mouth radius of these conical cavities can be assumed to be approximately half of the mean arithmetic roughness value, R_a. This prediction then implies that the surface modifications should result in microscale indentations or protrusions, with an R_a value of 0.7−2.8 μm, for potential heat transfer enhancement.

The main goal in this study was to utilize practical surface modification techniques that effectively increase roughness and to emphasize their potential effect on high heat flux, low superheat thermal management schemes involving liquid−vapor phase change. Two types of surfaces with microscale features were prepared and characterized, and their performance was evaluated against a reference smooth surface for heat transfer enhancement.

2. SURFACE PREPARATION AND EVALUATION METHODS

Two surface preparation methods were employed to modify initially plain, machine-finished smooth surface, and this surface served as the heat transfer surface of the heater sample (Figure 1b). Heaters were made of Al 6061 mainly because of their compatibility with the coolant. The first method involved removing material via particle blasting, and the resulting surface structure was called micro-indentations (mi). The second method involved adding material via plasma spray coating, and the corresponding surface structure was called microprotrusions (mp). In addition to being commercially available, well established, and economical, these methods also allow scaling up the heat transfer surface with acceptable uniformity of surface characteristics. The descriptions of all samples are summarized in Table 1, where the designations "-f", "-m", and "-c" in the sample identifications denote "fine", "medium", and "coarse" roughness levels, respectively.

2.1. Surface Modification by Particle Blasting. The first surface modification method was the surface blasting using particles by a

Table 1. Sample Descriptions

sample	surface condition, enhancement type, structure geometry, structure size
s	smooth, plain, machine-finished ($R_a \approx 0.3$ μm)
mi-f	microstructured, indentations, fine ($R_a \approx 2.1$ μm)
mi-m	microstructured, indentations, medium ($R_a \approx 3.2$ μm)
mi-c	microstructured, indentations, coarse ($R_a \approx 4.6$ μm)
mp-f	microstructured, protrusions, fine ($R_a \approx 4.2$ μm)
mp-m	microstructured, protrusions, medium ($R_a \approx 12.1$ μm)
mp-c	microstructured, protrusions, coarse ($R_a \approx 19.5$ μm)

dx.doi.org/10.1021/am402512f | ACS Appl. Mater. Interfaces 2013, 5, 9572−9578

siphon style nozzle gun. In this process, irregular shaped SiC and steel particles in the size ranges of fine (25−89 μm), medium (67−178 μm), and coarse (178−279 μm) were blasted on the surface of heater samples from a 25−30 mm distance using 515 kPa (60 psig) compressed air.

2.2. Surface Modification by Plasma Spray Coating. The other surface modification had been carried out by the atmospheric plasma spray coating technique using aluminum powder feedstock. Aluminum powder was selected considering its high thermal conductivity and good adhesion on Al 6061 substrate. The coating was deposited using three different powder feedstock with particle sizes of fine (<45 μm), medium (45−75μm), and coarse (75−140 μm) obtained from Valimet, U.S. All grades of powder were 99.7 wt % Al with slight impurities of Fe, Si, and Cu. Prior to the coating, a batch of heater samples was alumina grit (size 60 at 30 psi) blasted in order to increase the roughness of the surface to allow better adhesion of the coating. The plasma spray was conducted using a F4MB gun (Sulzer Metco, Westbury, NY, U.S.). Parameters for the plasma spray coating were optimized by varying the flow rates of powder, carrier gas, and primary gas in order to achieve a porous and rough surface of the deposit. Powders were injected externally in front of the spray gun using Ar as a carrier gas to deposit coating on Al 6061 substrates. Eventually, the deposition conditions listed in Table 2 were applied to coat the heat transfer surface of the heater samples.

Table 2. Plasma Spray Deposition Conditions

current (A)	voltage (V)	power (kW)	primary gas (slm [a])	secondary gas (slm [a])	carrier gas (slm [a])	standoff distance (mm)
500	44	22	42	2.4	2.8	120

[a]slm: standard liter per minute.

2.3. Microstructural Characterization. Microstructural characterization of the particle blasted and plasma spray coated surfaces was carried out using scanning electron microscopy (SEM, JEOL 6400F and Zeiss ULTRA-55). The 3D images of the surface indentation/protrusion and surface roughness of the samples were determined by confocal scanning laser microscope (Olympus LEXT OLS3100).

2.4. Heat Transfer Measurement. Once the samples were prepared and characterized, their performances were assessed through the heat transfer tests involving a high heat flux spray cooling technique. Experiments were conducted in a closed loop system that uses anhydrous ammonia as the coolant. Main components of this cooling system were a reservoir, a spray module, a condenser, and a pump. Designs of the spray module and the heater are shown in Figure 1. The spray module, manufactured by RINI Technologies, Inc., U.S., consists of three layers of liquid, vapor, and spray/exhaust manifolds and features two vapor-atomizing nozzles each covering half of the 1 cm × 2 cm heater area. In this type of nozzle, a fine liquid stream is injected into a high velocity vapor stream, and the shear force created by the vapor stream atomizes the liquid into fine droplets that are ejected through the nozzle orifice. The flow rates for ammonia liquid (1.6 mL cm^{-2} s^{-1}) and vapor (13.8 mL cm^{-2} s^{-1}) were held constant in the tests. The spray cooled heater side, i.e., heat transfer surface, was either a reference smooth surface or featured the microscale surface structures. Thick film resistors mounted on the back side of the heater were utilized to simulate and control heat load. Embedded thermocouples (TCs) inside the heater wall provided temperature monitoring during the tests. Heat transfer performance of different heater samples was evaluated by comparing the heater temperatures at the same heat flux levels. Details of the experimental setup and test conditions and procedure are described by Bostanci.[10]

3. RESULTS AND DISCUSSION

3.1. Microstructural Evaluation. Microstructural evaluation of the modified surfaces was made using SEM and confocal scanning laser microscope imaging. Figure 2 shows the microstructure of the smooth surface (s) and the surfaces

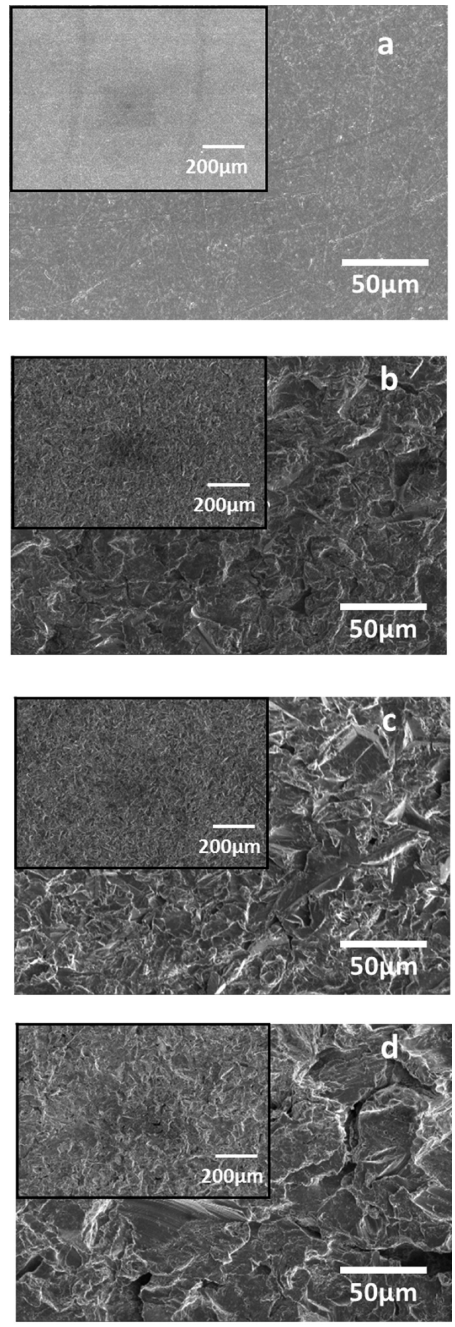

Figure 2. SEM images of the surfaces s (a), mi-f (b), mi-m (c), and mi-c (d) at ×100 (inset) and ×500 magnification.

with indentations at various roughness levels (mi-f, mi-m, mi-c) due to blasting. The change in the particle size of the blasting media creates a different size of impression, and hence variation in the surface roughness, attributed to the magnitude of the momentum. Parts a−c of Figure 3 are the SEM images illustrating the microstructure of the surfaces with protrusions (mp-f, mp-m, mp-c). These microsize protrusions vary with size and shape of the particles, their degree of melting in plasma flame, and subsequent splat formation on substrate upon impact. The protrusions offer many random sized re-entrant cavities, as indicated in Figure 3c. It is important to note that during the plasma spray, the substrate was not heated prior to the deposition which allows rapid cooling and splashing of the incoming molten particles on the substrate results in porous

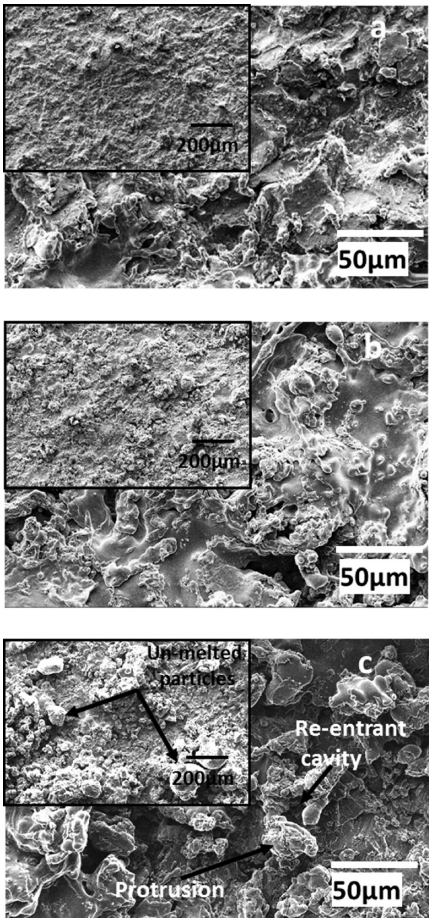

Figure 3. SEM images of the surfaces mp-f (a), mp-m (b), and mp-c (c) at ×100 (inset) and ×500 magnification.

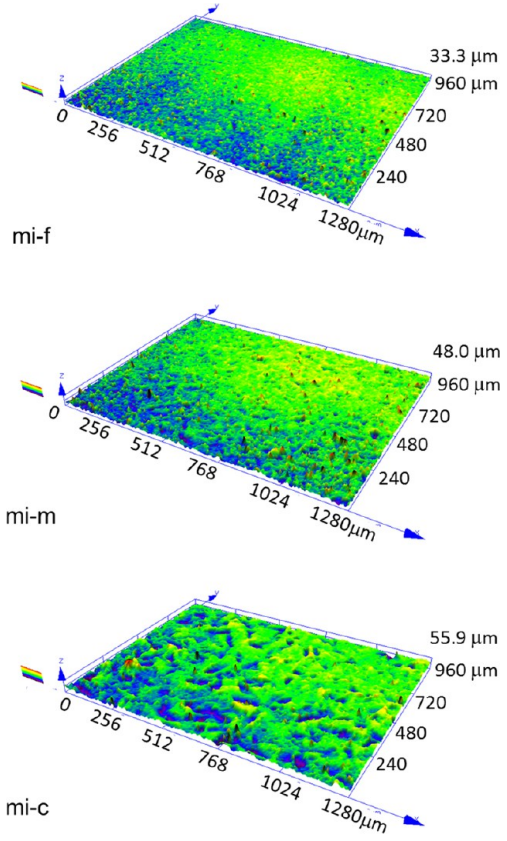

Figure 4. Confocal scanning laser microscope images of the surfaces mi-f, mi-m, and mi-c with dimensions in *x*, *y*, and *z* directions.

and rough deposition.[11] During the deposition process the melting behavior of the Al particles is quite different because of the size distribution.[12] For the constant plasma power, smaller particles fully melt and form a molten pool on the substrate for the partially melted incoming particles.[13] Figure 3 depicts the aforementioned behavior with size variation of the sprayed particles. The fine particles (<45 μm) melt completely and cause splashing on the substrate which contributes to the surface roughness (Figure 3a). The coating microstructure made of medium size particles (45−75 μm) illustrates the combination of both fully melted and semimolten particles (Figure 3b). In the case of a coating prepared by coarse powder (75−100 μm) the SEM microstructure shows a higher content of unmelted spherical particles along with a few fully melted particles (Figure 3c inset). In the present study, plasma spray parameters were kept constant for every feedstock powder. The resulting plasma was sufficient to melt smaller particles, while the larger particles remained partially melted and adhered to the molten pool of the fine particles on substrate, increasing surface roughness and re-entrant cavities (Figure 3c).

The 3D images of the surfaces from confocal scanning laser microscope enlighten more about the different surfaces. Figure 4 and Figure 5 include 3D images of the surfaces with indentations (mi-f, mi-m, mi-c) and protrusions (mp-f, mp-m, mp-c), taken by scanning an area of 1.28 mm × 0.96 mm. The roughness data based on the scanned surfaces are presented using statistical and extreme-value height descriptors in Figure 6 and Figure 7 along with their mathematical definitions. The most commonly used roughness parameter, arithmetic mean roughness (R_a), ranges between 0.3 μm for the surface s and 19.5 μm for the surface mp-c. The surfaces mp-f, mp-m, and mp-c in general have higher roughness than the surfaces mi-f, mi-m, mi-c. However, the R_a parameter alone would be misleading, since surfaces with widely different profiles, shapes, and frequencies can exhibit the same R_a value.[14] Thus, another parameter, mean height of roughness curve elements (R_c), was also calculated considering discrete peak-to-valley heights (Z_{ti}), and it basically confirmed the same trend. For even a broader view, extreme-value height descriptors, maximum peak height (R_p), maximum valley depth (R_v), and maximum roughness height (R_z), are useful. As shown in Figure 7, the deepest valley is 77.6 μm for the surface mp-c, while its maximum roughness height reaches 308.6 μm. In order to avoid occasional unrepresentative peaks and valleys in the characterization, a different roughness parameter, 10-point mean roughness (R_{zjis}), representing the highest five peaks and deepest five valleys, was also verified.

Another useful set of data obtained from the surface characterization with confocal laser scanning microscope was the actual surface area of the scanned section. This information was used to define an area enhancement factor EF_A as

$$EF_A = \frac{A_{surface}}{A_{projected}}$$

where $A_{surface}$ is the surface area and $A_{projected}$ is the projected area. Figure 8 plots EF_A values of all the microstructured surfaces. As can be expected, with increased roughness, available surface area for a fixed projected area increases.

dx.doi.org/10.1021/am402512f | ACS Appl. Mater. Interfaces 2013, 5, 9572−9578

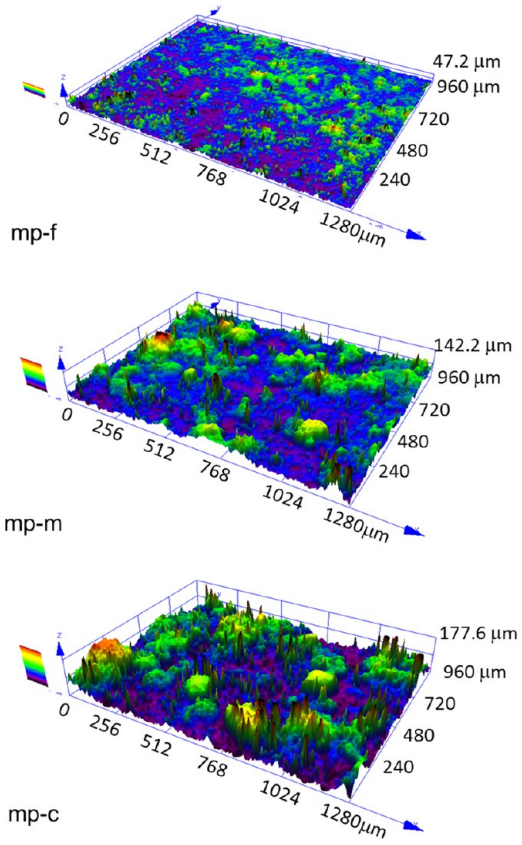

Figure 5. Confocal scanning laser microscope images of the surfaces mp-f, mp-m, and mp-c with dimensions in *x*, *y*, and *z* directions.

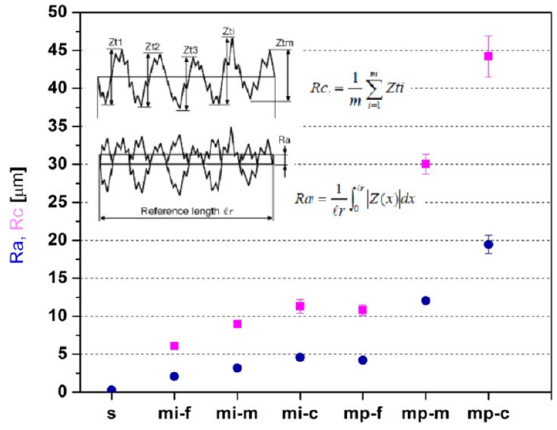

Figure 6. Roughness of microstructured surfaces with statistical height descriptors R_a and R_c (inset schematics and definitions adopted from Olympus confocal scanning laser microscope LEXT OLS3100/OLS3000 user's manual, version 6.0).

Data indicated that the area enhancement for the surface mp-c reaches 2.8. Since the microscope cannot effectively scan and capture the re-entrant cavities, these values for the surfaces mp-f, mp-m, and mp-c are conservative and believed to be even higher.

3.2. Heat Transfer Performance Evaluation. In order to evaluate the effect of surface modifications on heat transfer performance, the heater samples featuring the smooth and the two types of microscale surface structures were tested in the spray cooling system. On the basis of the performances of all the heater samples, the surfaces mi-f and mp-c provided the

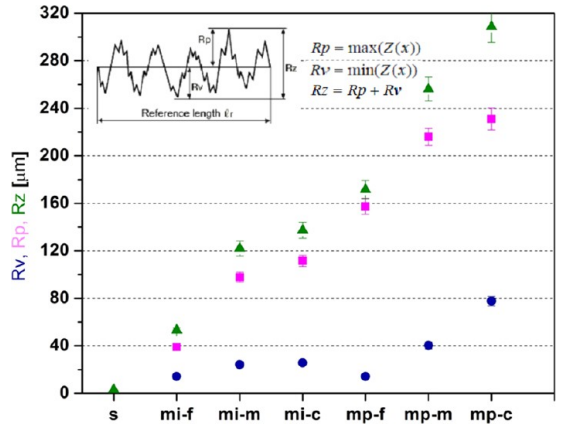

Figure 7. Roughness of microstructured surfaces with extreme-value height descriptors R_v, R_p, and R_z (inset schematics and definitions adopted from Olympus confocal scanning laser microscope LEXT OLS3100/OLS3000 user's manual, version 6.0).

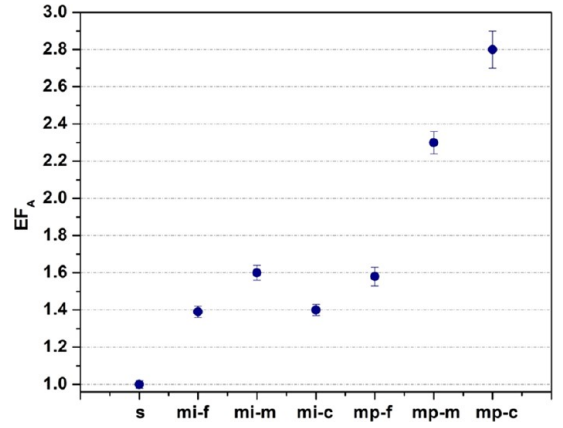

Figure 8. Area enhancement factor (EF_A) provided by microstructured surfaces.

best overall enhancement of microindentations and protrusions, respectively, and were reported in this study.

Figure 9, top, includes typical cooling curves that show surface superheat (ΔT_{sat}), defined as the difference between the surface temperature and the pool saturation temperature, as a function of heat flux (q''). During the tests, heat flux was gradually increased from 0 to 500 W/cm^2 in 50 W/cm^2 steps. Although the highest heat flux of 500 W/cm^2 in this study would represent the majority of today's high power applications, the system limitation, described with the critical heat flux (CHF) value, is much higher.[15] The baseline performance from the surface s indicates a 17 °C surface superheat at 500 W/cm^2 heat flux. At heat fluxes of >50 W/cm^2, both modified surfaces show greatly improved heat transfer rates where two-phase heat transfer mechanism starts to take place. It is well known that surface characteristics, including roughness, play an important role in promoting nucleate boiling heat transfer.[1−3] Particularly, surface cavities having the proper size range act as boiling nucleation sites and enhance heat transfer rate. In the low-to-middle heat flux range, the surface mp-c performs slightly better than the surface mi-f. Then in the middle-to-high heat flux range, the trend reverses. Better performance of the surface mp-c at lower heat fluxes might be attributed to the higher EF_A, along with abundant re-entrant cavities that can offer more available nucleation sites at

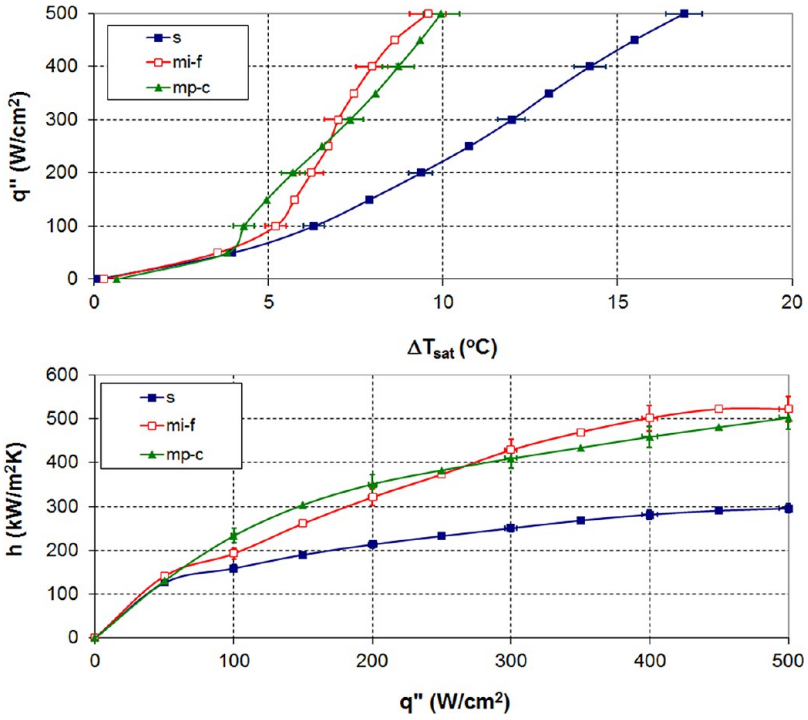

Figure 9. Heat transfer performance of the surfaces s, mi-f, and mp-c, when tested with an ammonia spray cooling system. Data illustrate ΔT_{sat} (surface superheat) and h (heat transfer coefficient) as a function of q'' (heat flux) with estimated uncertainty ranges. Both types of the microstructured surfaces provided significant heat transfer enhancement over the smooth surface.

a given surface superheat. However, the surface mp-c also yields some surface thermal resistance due to the added material, which plays a more important role at the higher heat fluxes. Another likely responsible mechanism in this range would be the level of free surface evaporation. A lower roughness with the surface mi-f is expected to result in a thinner liquid film retention that helps evaporation at the higher heat fluxes. At 500 W/cm^2, the surfaces mi-f and mp-c perform nearly the same and require a much lower surface superheat of 9.5−10 °C, compared to the surface s. Data from the other heater samples with microstructured surfaces are reported by Bostanci,[10] where the surface superheats varied within 2 °C in the middle heat flux range and within 1 °C in the high heat flux range.

As a common practice, heat transfer performance is evaluated with the heat transfer coefficient ($h = q''/\Delta T_{sat}$). Figure 9,bottom, shows heat transfer coefficients obtained from the three heater samples as a function of heat flux. The surface *s* yields an h value of 295 000 W m^{-2} K^{-1} at 500 W/cm^2, while the surfaces mp-c and mi-f reach to 500 000 and 520 000 W m^{-2} K^{-1}, respectively, presenting approximately 76% improvement over the baseline smooth surface. In order to put these h values in perspective, other commonly utilized cooling technologies can be considered for their respective performance. A typical natural convection with gases provides only 25 W m^{-2} K^{-1}, while a forced convection with liquids reaches 20 000 W m^{-2} K^{-1}, and microchannels involving phase change could achieve approximately 100 000 W m^{-2} K^{-1}.[16]

In practice, a well-designed spray cooling scheme can offer effective cooling for high power systems. Moreover, a specially prepared heat transfer surface such as the microstructured ones in this study can improve the cooling performance further for challenging thermal management applications such as power electronics and directed energy systems. Main benefits include lightweight and compact designs at system level, and higher efficiency and increased reliability at the component level.

4. CONCLUSIONS

In this study, two surface modification techniques have been investigated for heat transfer enhancement. Both particle blasting and plasma spraying are used to create microscale indentations and protrusions. For the surface *mp-c*, actual surface area available for heat transfer was increased up to 2.8× compared to the projected base area and the roughness (R_a) was increased up to 65× compared to the reference surface s. All the modified surfaces provided abundant cavities that act as active nucleation sites in boiling heat transfer. When the three heater samples were tested in an ammonia spray cooling system under high heat flux conditions, it was found that the microstructured surfaces were able to remove the same level of heat fluxes (>50 W/cm^2) with lower surface superheats, representing lower device temperatures. The best performance, obtained with the surface mi-f, resulted in up to 76% higher heat transfer coefficients at 500 W/cm^2 compared to the surface s. Hence, this study demonstrates a simple surface modification approach for compact and efficient design of high power thermal management systems.

AUTHOR INFORMATION

Corresponding Author

*E-mail: huseyin.bostanci@unt.edu.

Present Addresses

[⊥]H.B.: Department of Engineering Technology, University of North Texas, Denton, TX 76207.

[#]V.S.: Schlumberger, Rosharon, TX 77183.

Notes

The authors declare no competing financial interest.

■ ACKNOWLEDGMENTS

We acknowledge Air Force Research Laboratory (AFRL) Propulsion Directorate and Universal Technology Corporation for their financial support.

■ REFERENCES

(1) Carey, V. P. *Liquid−Vapor Phase-Change Phenomena*, 2nd ed.; Taylor and Francis: New York, 2008.
(2) Webb, R.; Kim, N. H. *Principles of Enhanced Heat Transfer*, 2nd ed.; Taylor and Francis: New York, 2005.
(3) Thome, J. R. *Enhanced Boiling Heat Transfer*; Taylor and Francis: New York, 1990.
(4) El-Genk, M. S.; Ali, A. F. *Int. J. Multiphase Flow* **2010**, *36*, 780−792.
(5) Yang, Y.; Ji, X.; Xu, J. *Int. J. Therm. Sci.* **2010**, *49*, 1227−1237.
(6) Tang, Y.; Tang, B.; Li, Q.; Qing, J.; Lu, L.; Chen, K. *Exp. Ther. Fluid Sci.* **2013**, *44*, 194−198.
(7) Wu, W.; Bostanci, H.; Chow, L. C.; Hong, Y.; Su, M.; Kizito, J. P. *Int. J. Heat Mass Transfer* **2010**, *53*, 1773−1777.
(8) Betz, A. R.; Jenkins, J.; Kim, C.-J. C.; Attinger, D. *Int. J. Heat Mass Transfer* **2013**, *57*, 733−741.
(9) Hsu, Y. Y. *J. Heat Transfer* **1962**, *84*, 207−213.
(10) Bostanci, H. High Heat Flux Spray Cooling with Ammonia on Enhanced Surfaces. Ph.D. Dissertation, University of Central Florida, Orlando, FL, 2010.
(11) Pawlowski, L. *The Science and Engineering of Thermal Spray Coatings*, 2nd ed.; John Wiley & Sons: New York, 2008.
(12) Suresh Babu, P.; Rao, D. S.; Rao, G. V. N.; Sundararajan, G. *J. Therm. Spray Technol.* **2007**, *16*, 281−290.
(13) Bakshi, S. R.; Singh, V.; Seal, S.; Agarwal, A. *Surf. Coat. Technol.* **2009**, *203*, 1544−1554.
(14) Bhushan, B. *Introduction to Tribology*; John Wiley & Sons: New York, 2002.
(15) Bostanci, H.; Rini, D. P.; Kizito, J. P.; Singh, V.; Seal, S.; Chow, L. C. *Int. J. Heat Mass Transfer* **2012**, *55*, 3849−3856.
(16) Cengel, Y. *Heat Transfer: A Practical Approach*, 2nd ed.; McGraw-Hill: New York, 2002.